TREND

Trapped Radiation Environment Model Development

Time Dependent Radiation-Belt Space Weather Modelling

ESA/TOS-EMA Contract No. 11711/95/NL/JG - CCN 1 to Work Order No. 3

Technical Note 2C/2D

Description of the low-altitude proton model and model evaluation

M. Kruglanski and D. Heynderickx
(not complete)

B.I.R.A. – I.A.S.B.	D.E.R.T.S.	P.S.I.
Avenue Circulaire 3 B-1180 Brussel Belgium	ONERA CERT BP 4025 F-31055 Toulouse cedex 4 France	Laboratory for Astrophysics CH-5232 Villigen Switzerland

ESA Technical Management: E.J. Daly (WMA)

Chapter 1

Model description

This chapter is dedicated to a general description of a time-dependent model for low-altitude trapped protons based on the integration of the Fokker-Planck equation and including most of the physical processes described in Sect. 2.2. Currently, such models are based on a dipolar description of the magnetic field. Since the not dipolar components of the Earth's magnetic field have an important impact on the description of the trapped population at low altitudes, the proposed model is based on the set of IGRF magnetic field models. One should note that, with this choice, $L_m \neq L^*$, i.e. an explicit drift shell tracing is needed to evaluate the third invariant.

1.1 Plan analysis

In this section, we browse the main characteristics (coordinate system, time scales, boundary conditions, included physical processes) of our proposed time-dependent model for low-altitude trapped protons. In order to decrease the need in computer resources, the physical processes will be implemented with more or less accuracy relating to their role in the dynamic of trapped proton population at low altitudes. For instance, we will assume that the dependence of some of the physical processes on the proton energy can be separated from other dependences.

1.1.1 Coordinate system

Instead of the three adiabatic invariants, we have choose as coordinates the particle energy, the magnetic field intensity at the particle mirror points and the integral invariant function *I*. This choice is justified by the fact that

- the coulomb drag by atmospheric ionisation and excitation, which plays an important role for the modelling of the energetic low-altitude protons, only affects the particle energy (see Sect. 2.2.4);
- the magnetic drift shell are naturally labelled by the coordinate pair (I, B_m) in the guiding center approximation [1.1].

Since the Fokker-Planck equation has the form of Eq. (1.8) only when it is used with canonical coordinates, e.g. the three adiabatic invariants, Eq. (1.8) has to be transformed, for non-canon-

ical coordinates [1.2]. When the third invariant is assumed to be independent of the particle energy, the Jacobian for the transition between both set of coordinates is given by

$$G \equiv \frac{\partial(M, J, \Phi)}{\partial(E, B_m, I)} = \frac{E + m_0 c^2}{m_0 c^2} \frac{p}{B_m^2} \mathcal{L}\Phi \tag{1.1}$$

where $\mathcal{L}\Phi = I\, \partial\Phi/\partial I - 2B_m\, \partial\Phi/\partial B_m$. From Eq. (1.1) it stems the useful equalities

$$\frac{1}{G}\frac{\partial}{\partial E} G\ldots = \frac{1}{E + m_0 c^2}\left(2 + \frac{m_0^2 c^4}{p^2 c^2}\right) + \frac{\partial}{\partial E} \tag{1.2}$$

$$\frac{1}{G}\frac{\partial}{\partial B_m} G\ldots = \frac{-\frac{2I}{B_m}\frac{\partial\Phi}{\partial I} + I\frac{\partial^2\Phi}{\partial I \partial B_m} + 2\frac{\partial\Phi}{\partial B_m} - 2B_m\frac{\partial^2\Phi}{\partial B_m^2}}{\mathcal{L}\Phi} + \frac{\partial}{\partial B_m} \tag{1.3}$$

$$\frac{1}{G}\frac{\partial}{\partial I} G\ldots = \frac{\frac{\partial\Phi}{\partial I} + I\frac{\partial^2\Phi}{\partial I^2} - 2B_m\frac{\partial^2\Phi}{\partial I \partial B_m}}{\mathcal{L}\Phi} + \frac{\partial}{\partial I} \tag{1.4}$$

$$\frac{\partial}{\partial\Phi}\ldots = \frac{1}{\mathcal{L}\Phi}\left(\mathcal{L}\ldots - \frac{E(E + 2mc)}{E + mc}\frac{\partial\ldots}{\partial E}\right) \tag{1.5}$$

The quantities $\frac{\partial\Phi}{\partial I}, \frac{\partial\Phi}{\partial B_m}, \frac{\partial^2\Phi}{\partial I^2}, \frac{\partial^2\Phi}{\partial I \partial B_m}$ and $\frac{\partial^2\Phi}{\partial B_m^2}$ appearing in the above equations should evaluated numerically.

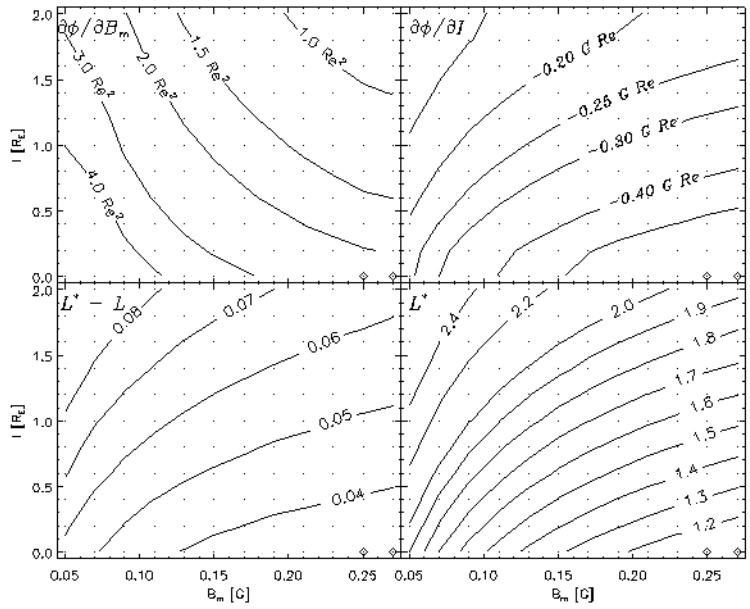

Fig. 1.1 Grid in the (B_m, I) space with contour plots relating to the third invariant.

As an example, the contours of $\partial\Phi/(\partial B_m)$, $\partial\Phi/(\partial I)$, $(L - L^*)$ and L^* in the (B_m, I) space are shown on Fig. 1.1 for IGRF 1995. The plots are obtained from a grid of 132 points, each one for which a magnetic drift shell has been traced.

1.1.2 Time scales

Different time scales take part in the physical description of the trapped proton population. The proposed model is intended to describe the long-term evolution of the population and short time variation will be averaged, e.g. daily variation. Note that the Fokker-Planck equation already includes an average over the gyration, bounce and drift motion. For the low-altitude trapped proton, the time variation of their population are linked to the variation of the atmospheric conditions and of the Earth's geomagnetic field.

Geomagnetic field variation

Since the proposed model is restricted to the low altitudes, we limit the description of the geomagnetic field to the part due to internal sources. It is generally admitted that this internal part is well represented by the IGRF magnetic field model. The secular variation of the geomagnetic field implies that the magnetic drift shells have to be traced for different epochs. In order to limit the computer time, the drift shells will only be traced at constant intervals of 5 years (1st of January 1980, 85, 90,...). All quantities to be averaged over a drift shell at a specific epoch, will be interpolated from their values evaluated at this fixed interval.

Atmospheric variations

Since the condition and composition of the Earth's atmosphere fluctuate with daylight hours and the solar activity, the time scale of the atmospheric variations extends from few hours to several month. For our application, we plan to average the atmospheric quantities over a 24 hours and to only evaluate them for a single day per season (e.g. 1st of January, April, July and October) but for a set of conditions of the solar and geomagnetic activity. For instance, four values of the solar radio flux F10.7 averaged over 90 days (e.g. 70, 100, 170 and 240) and three values of the planetary activity index Ap averaged over 30 days (e.g. 10, 20 and 45). For other days and conditions, the atmospheric quantities will be interpolated. This procedure should be equivalent to an average of all the processes with a time scale less than one or two months.

1.1.3 Boundary conditions

Different boundary conditions have to be stated in order to resolve the Fokker-Planck equation.

Energy range

The proton energy range is fixed to 1-300 MeV with the assumption that the proton flux cancels out above 300 MeV.

Altitude and shell parameter range

In the (B_m, I) space, each point is associated to a magnetic drift shell, the mirror points of which fluctuate as a function of the longitude. We assume that

- the proton flux cancels out for drift shells for which the altitude of the lowest mirror point is less than 100 km;
- the proton flux is given by an external model for drift shells for which the altitude of the lowest mirror point is greater than 3000 km, e.g. AP-8.

The first assumption is justified by the high efficiency of the atmospheric absorption at altitudes lower than 100 km. The contours of the lowest mirror point altitude in the (B_m, I) space are shown on Fig. 1.2 for the IGRF 1995 magnetic field model. The second boundary condition allows to limit the model to low altitudes as well as the physical processes to include in it.

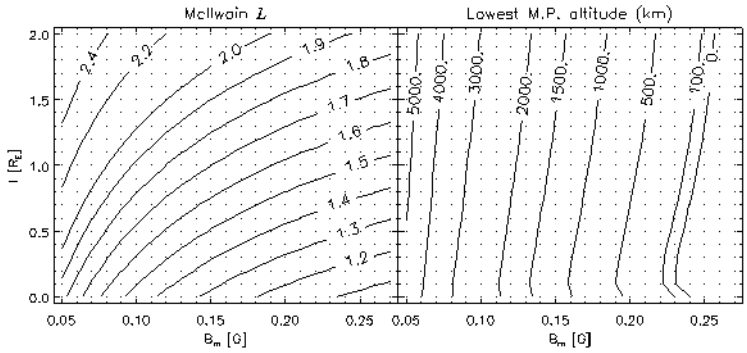

Fig. 1.2 Lowest mirror point altitude and L as function of (B_m, I)

We limit the (B_m, I) space by assuming that the proton flux at $L > 2$ is also given by an external model.

As shown by Fig. 1.2, the boundary conditions on the mirror point altitude and on the shell parameter limit approximately the model to I values less than 2.5 Earth's radii and to B_m values between 0.07 and 0.26 Gauss.

1.1.4 Magnetic field and atmospheric model

The model strongly depends on the choice of the magnetic field and atmospheric models since they are largely used to evaluate the physical processes. Since we restrict the model to low altitudes, we limit the description of the magnetic field to the geomagnetic IGRF/DRGF models, as already mentioned, which only depend on an epoch time, since they do not include the description of the external magnetic field.

We plan to use the atmospheric model MSISE but restricted to averaged values for few components (Hydrogen, Helium, Oxygen and Nitrogen). The restriction in the number of components is mainly justified by the fact that the atmospheric densities have to be combined to other physical quantities, e.g. nuclear cross section, data on which is not always available. The averaging of MSISE data will be obtained by an explicit average over the local time, and by the use of averaged driving parameters.

1.1.5 Drift shell averaging

To apply the Fokker-Planck formalism of Eq. (1.8), the different physical processes have to be average over the helicoidal particle trajectories associated to a given magnetic drift shell. In order to reduce the computer time, this average is related to the average of the physical processes over the magnetic drift shell surface. In this section, the averaging method is described, as well as, its application to the different physical processes.

Time averaging

In the adiabatic theory, the motion of a trapped particle is decomposed into the three components: gyration around the field line, bounce motion along field lines between conjugate mirror

points, and azimuthal drift. With the assumption that the three motions are independent, the time-average of a function $g(\mathbf{q})$ over a drift shell (I, B_m) can be written as

$$\langle g \rangle \equiv \frac{\circ g(\mathbf{q}) dt}{T} = \frac{g(\mathbf{q}) dt_1 dt_2 dt_3}{dt_1 dt_2 dt_3} \tag{1.6}$$

where the indices 1, 2 and 3 refer to the gyration, bounce and azimuthal drift motion, respectively, and $T = dt_3$ is the time needed to cover the drift shell. In the guiding-centre approximation, it can be shown [1.3] that Eq. (1.6) reduced to

$$\langle g \rangle = \frac{\mathcal{S}[g, B_m, I]}{\mathcal{S}[1, B_m, I]} \tag{1.7}$$

where the quantity $\mathcal{S}$ is defined as

$$\mathcal{S}[g, B_m, I] = g(\mathbf{q}) \frac{ds}{\sqrt{1 - B/B_m}} \frac{B^3 dl}{(2 - B/B_m)|\mathbf{B} \times \nabla B|} \tag{1.8}$$

In Eq. (1.8), the elements *ds* and *dl* correspond to length elements along the field line and azimuthal drift direction, respectively. The Eq. (1.8) can be evaluated by numericaly tracing the drift shell (I, B_m).

1.1.6 Source term

The source term will be limited to the CRAND effect (see Sect. 2.2.1) with a neutron leakage flux at 100 km only function of the geomagnetic latitude and neutron energy. The CRAND effect is evaluated over a drift shell by a simple ray tracing technique. It is determined by the injection rate $q(E, L, \alpha_0)$ of Eq. (2.2) and given by

$$p^2 S = \frac{S_n(E) \times \mathcal{S}[\circ J_n(\lambda) \Phi_n(\phi) d\beta, B_m, I]}{2\pi\, t_n\, \mathcal{S}[1, B_m, I]} \tag{1.9}$$

where the dependence on the energy, geomagnetic latitude and zenith angle of the neutron leakage flux has been separated. The geomagnetic latitude, zenith angle and energy dependences are given by

$$J_n(\lambda) = 0.0905 + \frac{0.731}{(1 + \exp[17.3 - 0.313\ \lambda])^{0.262}} \tag{1.10}$$

$$\Phi_n(\phi) = \frac{[2\pi\ \ln(7/3)]^{-1}}{3/4 + \cos\phi} \tag{1.11}$$

$$S_n = \frac{1}{0.4695}\begin{cases} 0.0155(E/5)^{-0.75} & \text{when } E \le 5 \\ 0.0155(E/5)^{-1.96} & \text{when } 5 \le E < 15 \\ [1.8(100-E)+0.3(E-15)]/85000 & \text{when } 15 \le E < 100 \\ 0.0003(E/100)^{-2.7} & \text{when } E \ge 100 \end{cases} \quad (1.12)$$

where J_n, Φ_n, S_n, λ and E are expressed in $\mathrm{cm}^{-2}\mathrm{s}^{-1}$, sr^{-1}, MeV^{-1}, degrees and MeV, respectively. Note that in Eq. (1.9), the geomagnetic latitude and the zenith angle are function of the location **q** along the drift shell, the local magnetic field and the azimuthal angle β.

1.1.7 Loss terms

The loss term will include the nuclear inelastic interaction effects (see Sect. 2.2.2). They are evaluated over a drift shell with the help of MSISE and tabulated cross sections. The charge exchange effects are neglicted since they accour at energies less than 1 MeV. It is determined by the nuclear inelastic cross sections σ_O and σ_N of Eq. (2.4), and is given by

$$Q = \frac{\sqrt{E(E+2m_0c^2)}}{E+m_0c^2}\sum_i \sigma_i(E)\frac{\mathcal{S}[\rho_i, B_m, I]}{\mathcal{S}[1, B_m, I]} \quad f(E, B_m, I) \quad (1.13)$$

where the sum covers over the two atmospheric constituents.

Note that an additional pseudo lost term is included by the boundary condition at very low altitudes.

1.1.8 Friction term

The friction term will include the stopping power due to excitation and ionization of atmospheric constituents (see Sect. 2.2.4). They will be also evaluated over a drift shell with the help of MSISE model.

Diffusion term

The diffusion term will be limited to an analytical expression that varies as L^{*10}, and which can be evaluated using Eq. (1.5).

References

[1.1] Roederer, J.G., 1970: Dynamics of Geomagnetically Trapped Radiation, Springer-Verlag

[1.2] Schulz, M., 1991: The Magnetosphere, in Geomagnetism, vol. 4, ed. P. Jacobs, Academic Press, 87-293

[1.3] Heynderickx, D., M. Kruglanski and J. Lemaire, 1996: A New Tool for Calculating Drift Shell Averaged Atmospheric Density, AGU Monograph 97, 173–178